Journal of Biomechanics 43 (2010) 945–952

Contents lists available at ScienceDirect

Journal of Biomechanics

journal homepage: www.elsevier.com/locate/jbiomech
www.JBiomech.com

Simultaneous prediction of muscle and contact forces in the knee during gait

Yi-Chung Lin [a], Jonathan P. Walter [a], Scott A. Banks [a,b], Marcus G. Pandy [c], Benjamin J. Fregly [a,b,c,d,*]

[a] Department of Mechanical & Aerospace Engineering, 231 MAE-A Building, P.O. Box 116250, University of Florida, Gainesville, FL 32611-6250, USA
[b] Department of Orthopaedics and Rehabilitation, University of Florida, Gainesville, FL, USA
[c] Department of Mechanical Engineering, University of Melbourne, Melbourne, Australia
[d] Department of Biomedical Engineering, University of Florida, Gainesville, FL, USA

ARTICLE INFO

Article history:
Accepted 31 October 2009

Keywords:
Musculoskeletal model
Muscle force
Contact force
Inverse dynamic optimization
Biomechanics

ABSTRACT

Musculoskeletal models are currently the primary means for estimating *in vivo* muscle and contact forces in the knee during gait. These models typically couple a dynamic skeletal model with individual muscle models but rarely include articular contact models due to their high computational cost. This study evaluates a novel method for predicting muscle and contact forces simultaneously in the knee during gait. The method utilizes a 12 degree-of-freedom knee model (femur, tibia, and patella) combining muscle, articular contact, and dynamic skeletal models. Eight static optimization problems were formulated using two cost functions (one based on muscle activations and one based on contact forces) and four constraints sets (each composed of different combinations of inverse dynamic loads). The estimated muscle and contact forces were evaluated using *in vivo* tibial contact force data collected from a patient with a force-measuring knee implant. When the eight optimization problems were solved with added constraints to match the *in vivo* contact force measurements, root-mean-square errors in predicted contact forces were less than 10 N. Furthermore, muscle and patellar contact forces predicted by the two cost functions became more similar as more inverse dynamic loads were used as constraints. When the contact force constraints were removed, estimated medial contact forces were similar and lateral contact forces lower in magnitude compared to measured contact forces, with estimated muscle forces being sensitive and estimated patellar contact forces relatively insensitive to the choice of cost function and constraint set. These results suggest that optimization problem formulation coupled with knee model complexity can significantly affect predicted muscle and contact forces in the knee during gait. Further research using a complete lower limb model is needed to assess the importance of this finding to the muscle and contact force estimation process.

1. Introduction

When the human musculoskeletal system is impaired, mobility is often limited, leading to a decreased quality of life (Praemer et al., 1999). Common clinical examples include osteoarthritis, patellofemoral pain, stroke, cerebral palsy, and paraplegia. Knowledge of *in vivo* muscle and joint contact forces during normal and pathological walking would assist clinicians in diagnosing musculoskeletal disorders and developing new or improved treatments. Since direct measurement of these internal forces is not clinically feasible, musculoskeletal modeling has become the primary approach for developing estimates (Anderson and Pandy, 2003; Neptune et al., 2004; Buchanan et al., 2005; Jinha et al., 2006; Shelburne et al., 2006; Liu et al., 2008; Besier et al., 2009). However, because of the "muscle redundancy problem" (i.e., more muscles than degrees-of-freedom in the skeletal model) (Crowninshield, 1978), estimates of *in vivo* muscle and contact forces during gait remain largely unvalidated, particularly for the knee where multiple bones articulate over multiple surfaces.

Recent *in vivo* contact force measurements made with instrumented knee implants provide an opportunity for quantitative evaluation of muscle and contact force estimates during gait (Kaufman et al., 1996; Taylor et al., 2004; D'Lima et al., 2005a, 2005b, 2006). Since muscle forces are the primary determinants of joint contact forces (Anderson and Pandy, 2003; Herzog et al., 2003; Shelburne et al., 2004), accurate estimates of joint contact forces would imply reasonable estimates of muscle forces. To date, musculoskeletal modeling studies that estimated *in vivo* tibial contact forces during gait have used a sequential (or two-stage) computational approach (Taylor et al., 2004; Shelburne et al., 2005; Kim et al., 2009). In the first stage, muscle forces

* Corresponding author at: Department of Mechanical & Aerospace Engineering, 231 MAE-A Building, P.O. Box 116250, University of Florida, Gainesville, FL 32611-6250, USA. Tel.: +1 352 392 8157; fax: +1 352 392 7303.
E-mail address: fregly@ufl.edu (B.J. Fregly).

0021-9290/$ - see front matter © 2009 Elsevier Ltd. All rights reserved.
doi:10.1016/j.jbiomech.2009.10.048

were estimated using a musculoskeletal model without articular contact, where muscle redundancy was resolved using inverse dynamic (i.e., static) or forward dynamic optimization. In the second stage, contact forces were estimated by applying the estimated muscle forces to a separate articular contact model (Kim et al., 2009) or static equilibrium model in the superior–inferior direction (Taylor et al., 2004; Shelburne et al., 2005). Articular contact models were omitted in the first stage presumably due to their high computational cost and complexity (Bei and Fregly, 2004).

This sequential approach possesses three important limitations, all of which stem from the lack of an articular contact model in the first stage. First, it does not utilize all available inverse dynamic loads as constraints when static optimization is used. Of the six inverse dynamic loads acting on the tibia, only those to which contact forces are assumed not to contribute can be used as constraints. Usually only the net flexion–extension torque is assumed to fulfill this requirement (e.g., Anderson and Pandy, 2001), and consequently the feasible solution space is not narrowed to the fullest extent possible. Second, it assumes that contact forces do not affect muscle forces (though muscle forces are assumed to affect contact forces). Though one study has proposed minimization of compressive contact forces for muscle force estimation (Schultz and Andersson, 1981), such a criterion cannot be investigated using the sequential approach. Third, it requires assumptions about patellar motion in the first stage. These assumptions may be inconsistent with the patellar motion (and hence quadriceps moment arms) predicted in the second stage, thereby affecting the estimated muscle and contact forces.

This study takes a fundamentally different approach by estimating muscle and contact forces *simultaneously* in the knee during gait. A single three-dimensional knee model combining muscle, articular contact, and dynamic skeletal models is used to develop the estimates. Two contacts (medial and lateral) are modeled for the tibiofemoral (TF) joint and one contact for the patellofemoral (PF) joint. The high computational cost and complexity of articular contact models is eliminated by using "fast" surrogate contact modeling techniques (Lin et al., 2006, 2008, 2009). Muscle redundancy is resolved using static optimization with two cost functions and four constraint sets to investigate how optimization problem formulation affects the calculated muscle and contact forces. Medial and lateral contact force estimates are evaluated quantitatively using *in vivo* tibial contact force measurements obtained from the same subject (Zhao et al., 2007a). Our hypotheses were that the model would be able to reproduce all available *in vivo* contact force and inverse dynamic data simultaneously and that muscle and contact forces estimated by the two cost functions would become more similar as more inverse dynamic loads were used as constraints.

2. Methods

2.1. Experimental data collection

Previously reported experimental gait data collected from an adult male subject implanted with an instrumented knee replacement (age 80, mass 68 kg, height 1.7 m, right knee, neutral alignment) eight months after surgery were used for this study (Zhao et al., 2007a,b). Institutional review board approval and patient informed consent were obtained.

The subject performed two types of gait tasks. The first type was treadmill gait under fluoroscopic motion analysis and the second was overground gait under video motion analysis (Motion Analysis Corporation, Santa Rosa, CA) with simultaneous collection of ground reaction data (AMTI Corporation, Watertown, MA). Instrumented knee data were collected simultaneously in both cases. One overground gait trial with cadence closest to the fluoroscopic gait data was selected for subsequent analysis.

The subject was implanted with a first-generation instrumented knee design (D'Lima et al., 2005b). The implant consisted of four uniaxial force transducers, a micro transmitter, and an antenna. The distribution of contact forces between the medial and lateral compartments was calculated from the four force transducer measurements using validated regression equations (Zhao et al., 2007a).

2.2. Musculoskeletal model development

A 12 degree-of-freedom (DOF) patient-specific knee model actuated by eleven muscles and possessing TF and PF articular contact (Fig. 1) was constructed to calculate muscle and contact forces simultaneously for the instrumented knee. The femur in the knee model was fixed to ground, while the tibia and patella were allowed to move relative to it via two separate 6 DOF joints (i.e., 3 translations and 3 rotations). The equations of motion for the model were derived using Autolev symbolic manipulation software (OnLine Dynamics, Sunnyvale, CA). Three-dimensional TF and PF contact models were constructed using "fast" surrogate contact modeling techniques (Lin et al., 2006, 2008, 2009). These models reproduced 6 DOF load-displacement relationships sampled from elastic foundation (EF) contact models of the subject's implant components created from three-dimensional CAD geometry with linear elastic material properties (Bei and Fregly, 2004). The complete knee model was implemented in Matlab (The Mathworks, Natick, MA).

The eleven muscles included in the model were as follows: vastus medialis (VM), vastus lateralis (VL), vastus intermedius (VI), rectus femoris (RF), semimembranosus (SM), semitendinosus (ST), biceps femoris long head (BFLH), biceps femoris short head (BFSH), tensor fascia latae (TFL), gastrocnemius medial head (GM), and gastrocnemius lateral head (GL). Based on Anderson and Pandy (2001), the force generated by each muscle was modeled as an activation times a peak isometric strength, where strength values were taken from Kim et al. (2009). Each muscle was activated independently except for medial hamstrings (same activation signal for SM and ST) and vasti (same activation signal for VM, VI, and VL), resulting in eight activation signals. The patellar ligament was represented by three parallel linear springs with a total stiffness of 2000 N/mm (Reeves et al., 2003). Other knee ligaments were omitted from the model.

Construction of the 12 DOF knee model involved registering a patient-specific inverse dynamic skeletal model to a patient-specific geometric implant/bone model. The geometric model was constructed from the patient's post-surgery CT data, CAD models of the patient's implant components, and MR-derived bone models from a different subject of comparable stature (Banks et al., 2005; Kim et al., 2009) (Fig. 2). This model provided muscle and patellar ligament origin and insertion locations along with implant component locations within the bones. The inverse dynamic model was constructed using the patient's overground gait data and additional isolated joint motion trials processed within established patient-specific model creation software (Reinbolt et al., 2005, 2008). This model provided net loads (i.e., three forces and three torques) acting on the instrumented tibia during overground gait. The thigh and shank in the inverse dynamic model were registered to the femur and tibia/fibula in the geometric model by finding the best-fit alignment between corresponding joint centers (ankle, knee, and hip) and two additional points on corresponding knee functional axes (Fig. 3). The functional

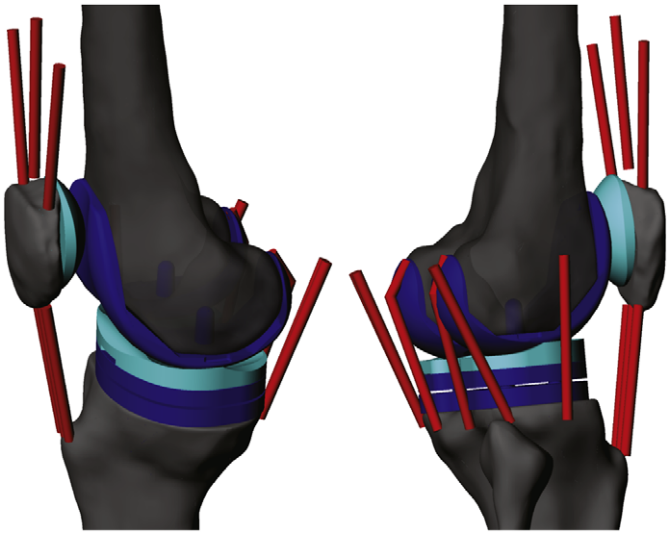

Fig. 1. Twelve degree-of-freedom knee model combining muscle, articular contact, and dynamic skeletal models. The model is controlled by 11 muscles and incorporates tibiofemoral and patellofemoral contact. Compressive contact force on the tibia (patella) is defined as the component of net contact force acting perpendicular to the planar back surface of the polyethylene tibial insert (patellar button).

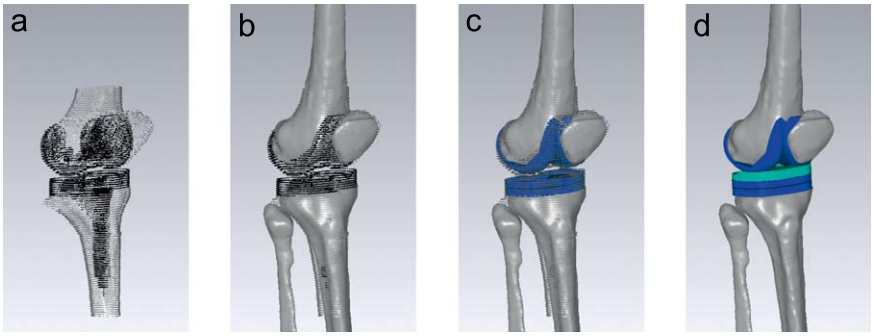

Fig. 2. Visual depiction of the steps involved in creating the patient-specific implant/bone geometric model. (a) Segmentation of implant components and bones from post-surgery CT data. (b) Alignment of MR-derived bone models from a different subject with the segmented bones. (c) Alignment of metallic implant CAD models to the segmented implant components. (d) Positioning of polyethylene implant components on tibial baseplate and patella and deletion of segmented points. All geometry registration was performed using Geomagic Studio (Raindrop Geomagic, Research Triangle Park, NC).

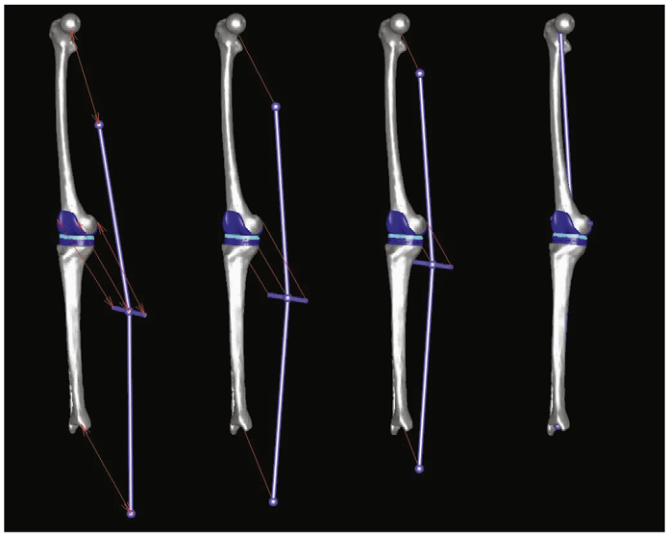

Fig. 3. Animation sequence (left to right) of the static analysis used to register the patient-specific full-leg inverse dynamic model to the patient-specific implant-bone geometric model. Five stiff springs (dotted lines) between corresponding anatomic points were used to pull the inverse dynamic model onto the geometric model.

axis for the geometric model was determined from the fluoroscopic motion data and for the inverse dynamic model from the video motion data.

2.3. Muscle and contact force estimation

The 12 DOF patient-specific knee model was used to estimate muscle and contact forces simultaneously using a two-level optimization approach. For each time frame during the gait cycle, an outer-level muscle force optimization modified design variables related to muscle activations while an inner-level pose optimization modified design variables related to tibial and patellar pose on the femur. Given the current guess at the muscle activations, the inner-level optimization found the resulting static configuration and returned the cost function and constraints required by the outer-level optimization. Both optimizations were performed using a Matlab nonlinear least-squares algorithm, with constraints being treated as penalty terms in an augmented cost function so that inability to meet them would not cause the optimization to fail.

The outer-level optimization used two cost functions and four constraint sets to investigate how optimization problem formulation affects the calculated muscle and contact forces (Glitsch and Baumann, 1997; Jinha et al., 2006). The two cost functions were minimization of the sum of the squares of muscle activations (Kaufman et al., 1991; Anderson and Pandy, 2001) and minimization of the sum of the three compressive contact forces (medial tibiofemoral, lateral tibiofemoral, and patellofemoral) (Schultz and Andersson, 1981), where the direction of compressive contact force was perpendicular to the planar back surface of the tibial insert or patellar button. The four constraint sets were composed of different combinations of three residual loads acting on the tibia (Table 1). Residual loads represent the differences between the calculated inverse dynamic loads and the loads produced by the combined effect of muscle, contact, and ligament forces. The remaining three residual loads acting on the tibia along with all six residual loads acting on the patella were minimized as part of the inner-level pose optimization.

Table 1
Summary of the four optimization constraints sets composed of different combinations of three tibial residual loads. Residual loads are for the flexion–extension torque ($T^{Residual}_{Tibia\ FE}$), the anterior–posterior force ($F^{Residual}_{Tibia\ AP}$), and the internal–external torque ($T^{Residual}_{Tibia\ IE}$). The residual flexion–extension torque was included in all four constraint sets since it is the most commonly used constraint for predicting muscle forces at the knee.

Constraint set	$T^{Residual}_{Tibia\ FE}$	$F^{Residual}_{Tibia\ AP}$	$T^{Residual}_{Tibia\ IE}$
1	✓		
2	✓	✓	
3	✓		✓
4	✓	✓	✓

The eight outer-level optimization problem formulations were solved two ways – with and without additional constraints to match the *in vivo* medial and lateral contact force measurements. Problems that included these constraints were termed "matched" formulations and were used to verify that muscle forces in the model spanned the solution space necessary to reproduce the *in vivo* contact force data. Problems that omitted these constraints were termed "predicted" formulations and were used to evaluate how well different optimization problems could predict the *in vivo* contact forces without knowing them a priori. One "matched" formulation (minimize sum of squares of muscle activations using constraint set 1) was used to verify that the muscle and contact force estimates generated using surrogate contact models matched those generated using the EF contact models from which the surrogate contact models were constructed. All optimization solutions were generated at 5% intervals throughout the gait cycle.

Additional details on *Musculoskeletal model development* and *Muscle and contact force estimation* can be found in the Supplementary Material section.

3. Results

Optimizations performed using the surrogate and EF contact models produced nearly identical motion, contact force, and muscle force results, as demonstrated by the one selected "matched" formulation. For the TF and PF joints, root-mean-square (RMS) differences in joint translations/rotations and contact forces/torques were less than 0.6 mm/0.7° and 4 N/0.3 Nm, respectively. Furthermore, both types of contact models reproduced the *in vivo* medial and lateral contact force measurements accurately, with RMS errors being less than

10 N. RMS differences in muscle force estimates generated by the two types of contact models were less than 15 N. While approximately 90 min (32 h) of CPU time were required to optimize one time frame (one complete gait cycle) using the EF contact models, only 2 min (42 min) were required when using the surrogate models.

The eight "matched" formulations accurately matched the *in vivo* medial and lateral contact force measurements while producing different muscle force estimates depending on the selected outer-level cost function and constraint set (Figs. 4 and 5). For all eight formulations, RMS errors between measured and predicted contact forces were on the order of 10 N, and worst-case RMS residual loads for the TF and PF joints were below 3 N and 1 Nm. The only exceptions were constraint sets 2 and 4, where RMS residual loads for anterior–posterior force were on the order of 100 N (see Supplementary Material). Unlike muscle forces, PF contact forces exhibited similar magnitudes and shapes for all eight problem formulations with a maximum force of approximately 250 N. RMS differences in muscle forces (PF contact forces) predicted by the two cost functions decreased as more inverse dynamic loads were added as constraints (Table 2 – top). None of the muscles exceeded its maximum isometric force except for BFSH and TFL.

The eight "predicted" formulations predicted medial tibial contact forces that were comparable and lateral tibial contact forces that were lower in magnitude compared to measured tibial contact forces (Fig. 6). Larger lateral contact forces were generated when more inverse dynamic loads than just the flexion–extension torque were used as constraints. One problem formulation (minimize sum of three compressive contact forces using constraint set 2) predicted the two *in vivo* peaks in medial and lateral contact force to within 29 N. Similar to the "matched" solutions, muscle forces exhibited large changes and PF contact forces small changes when the problem formulation was changed, with BFSH and TFL again being the only muscles to exceed their maximum isometric forces (Fig. 7). While PF contact forces were similar to the "matched" solutions, muscle forces exhibited noticeable differences in shape and magnitude (e.g., compare "predicted" and "matched" solutions for TFL, MGAS, and LGAS). In contrast to the "matched" solutions, RMS differences in muscle and PF contact forces predicted by the two cost functions did not decrease as more inverse dynamic loads were added as constraints, nor did RMS differences in medial and lateral contact forces (Table 2 – bottom).

4. Discussion

This study predicted muscle and contact forces simultaneously in the knee during gait using a knee model that combined muscle, articular contact, and dynamic skeletal models. To our knowledge, no previous study has included explicit articular contact models in the *in vivo* muscle force estimation process for the knee. Inclusion of contact models allowed us to eliminate assumptions about which inverse dynamic loads have little contribution from contact forces and to investigate cost functions utilizing tibiofemoral and patello-femoral contact forces. Muscle force estimates tended to be more sensitive to optimization problem formulation than were contact force estimates, with PF contact force being especially insensitive. These observations support the statement by Jinha et al. (2006) that "precise geometric representation of the musculoskeletal system [is needed] if general force-sharing rules are to be derived."

The simultaneous approach to muscle and contact force prediction used in this study was made possible by our recent development of surrogate contact modeling methods (Lin et al., 2006, 2008, 2009). While it is theoretically possible to employ EF contact models for the simultaneous approach, as demonstrated by the one selected "matched" formulation, 32 hours of CPU time

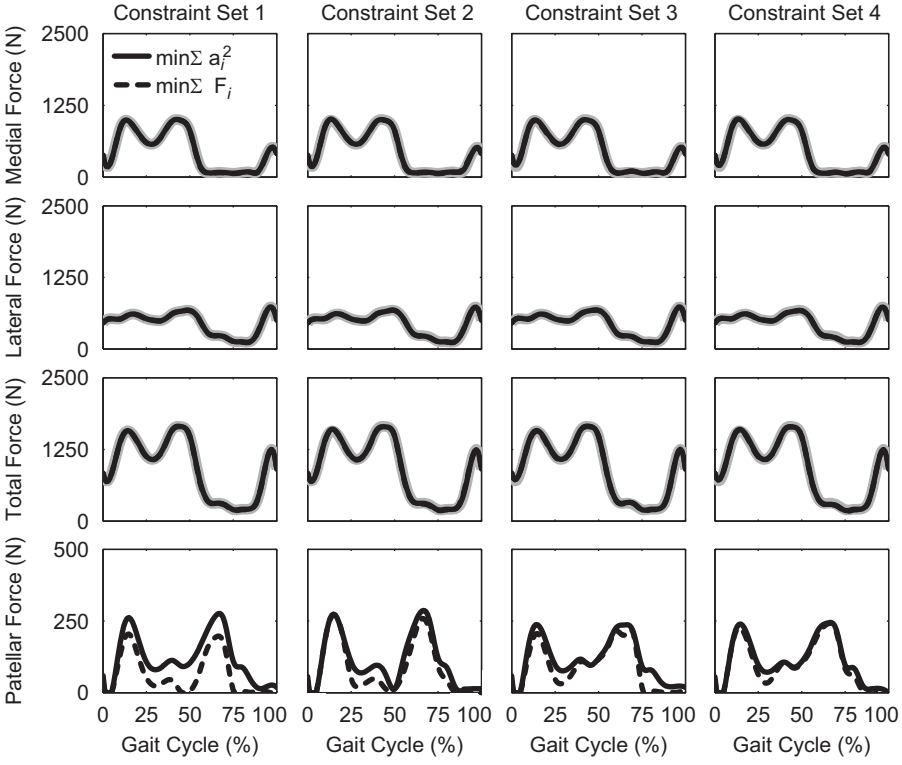

Fig. 4. Comparison of measured (gray bands) and estimated (solid and dotted lines) *in vivo* compressive contact forces for the eight "matched" optimization problems. Each column represents a different constraint set defined in Table 1. Estimates overlay *in vivo* measurements for medial, lateral, and total compressive contact force. No *in vivo* patellar compressive contact force measurements were available.

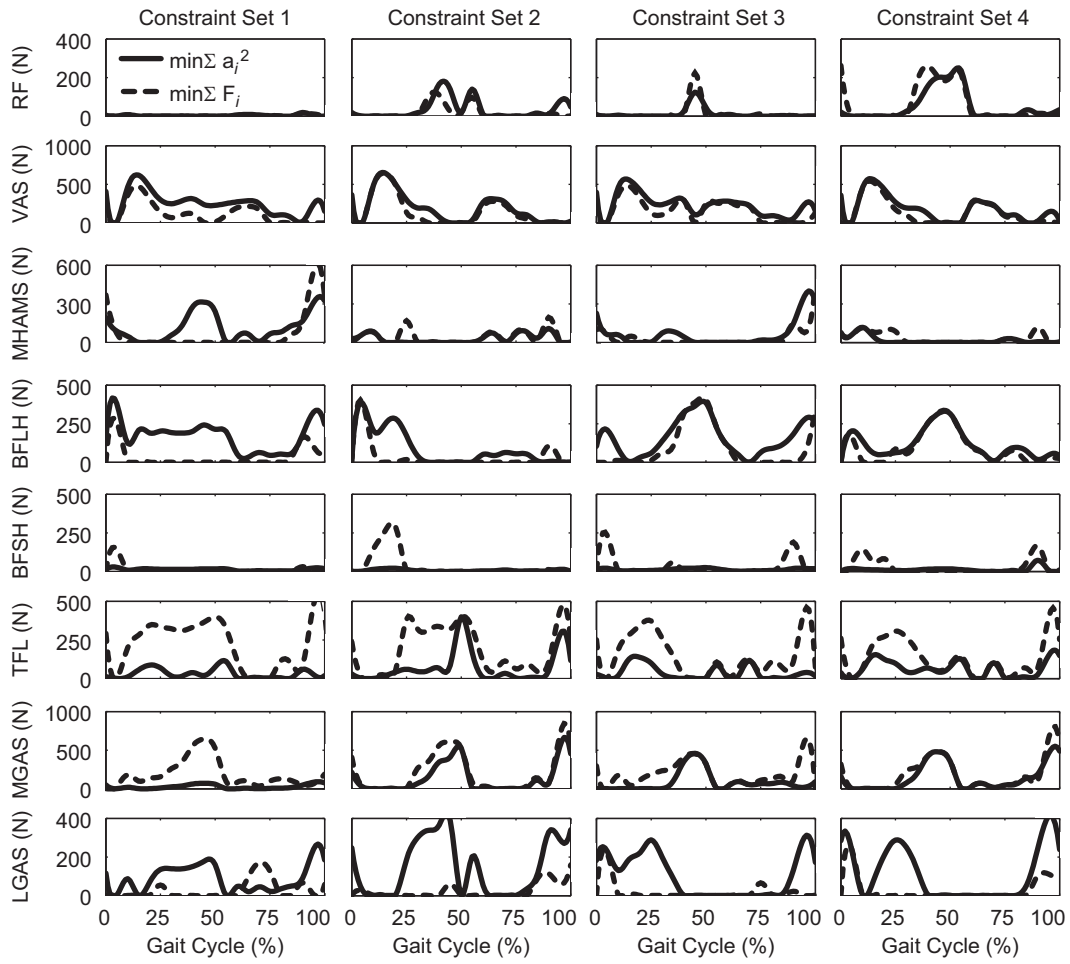

Fig. 5. Estimated muscle forces for the eight "matched" optimization problems. Each column represents a different constraint set defined in Table 1.

Table 2
Root-mean-square difference in solutions generated by the two cost functions as more inverse dynamic loads were added as constraints.

Constraint set	Muscle forces	Medial contact force	Lateral contact force	Total contact force	Patellar contact force
"Matched" solutions					
1	152.28	7.39	3.70	9.55	64.74
2	109.28	8.87	3.11	11.23	32.69
3	112.85	7.48	3.08	9.70	34.78
4	84.88	7.37	3.48	8.33	16.56
"Predicted" solutions					
1	44.67	104.34	92.98	44.52	12.17
2	86.91	231.24	134.41	277.76	42.63
3	74.74	40.47	77.02	93.68	27.31
4	72.83	146.71	122.22	233.25	48.80

per optimization is undesirable for performing repeated optimizations with different problem formulations. Though the computational cost of constructing the three surrogate contact models was on the order of 30 hours of CPU time, this cost was paid once initially and then quickly redeemed by the 42 min of CPU time required to solve the optimization problem over one full gait cycle.

Our PF contact force estimates exhibited similarities and differences with previously published estimates. Consistent with our study, Sharma et al. (2008) reported that patellar contact forces may be largely determined by TF contact forces. In contrast to our study, Ward and Powers (2004) reported maximum PF contact forces on the order of 400–800 N during gait as calculated by a simpler model. Our maximum values of approximately 250 N were lower, possibly because our model required fewer assumptions about the interactions between muscles and knee contact geometry.

None of the "predicted" problem formulations generated significant lateral contact force during midstance. A related modeling study by Kim et al. (2009) used a sequential approach and had a similar problem. To match *in vivo* lateral contact force measurements, the authors had to increase the pre-strain in the lateral collateral (LCL) and popliteofibular (PFL) ligaments until they generated approximately 400 N of lateral contact force during midstance. However, intraoperative measurement of medial and lateral tibial contact force during passive knee

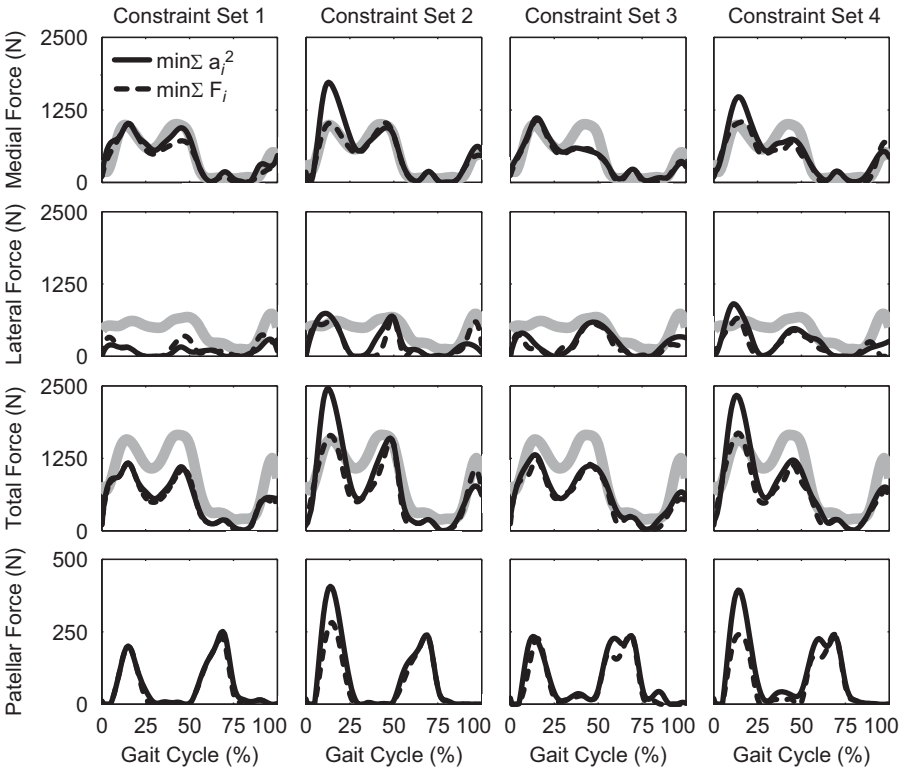

Fig. 6. Comparison of measured (gray bands) and estimated (solid and dotted lines) *in vivo* compressive contact forces for the eight "predicted" optimization problems. Each column represents a different constraint set defined in Table 1. No *in vivo* patellar compressive contact force measurements were available.

flexion suggests that collateral ligaments contribute only about 50 to 100 N of contact force on each side (D'Lima et al., 2007). Thus, omission of the LCL and PFL in our model is not a likely explanation for the "missing" lateral contact force. Other possible explanations are weak TFL and BFSH muscles, omission of certain muscles from our model (e.g., sartorius and gracilis), omission of neighboring joints in the model, predicted lateral muscle activations that may be inconsistent with the subject's actual activations (Winby et al., 2009), and uncertainty over the form of the optimization cost function.

The reliability of muscle and contact force estimates at the knee would likely be improved using a combination of optimization and EMG-driven methods (Lloyd and Besier, 2003; Buchanan et al., 2005; Besier et al., 2009; Winby et al., 2009). Additional experimental data provided by EMG measurements would make the "predicted" optimization solutions more unique. While knowing the "correct" optimization cost function would become less critical, a cost function would still be required to predict forces in muscles for which no EMG measurements are available. Since EMG data were not available for the present study, a new experimental data set is needed to investigate this possibility.

Though availability of *in vivo* contact force data provided a unique opportunity for evaluating knee muscle and contact force estimates, this study still possesses a number of limitations. First, only a single gait trial from a single subject was analyzed. Data from additional trials and subjects are needed to assess the extent to which these results can be generalized. Second, the patient used in this study had an implanted knee, so it is not known how well these results apply to subjects with natural knees. We anticipate, however, that the principles elucidated by this study will be applicable to natural knees as well. Third, ligaments (apart from the patellar ligament) and contact friction were not included in the model, which may be important for reducing residual loads in anterior–posterior tibial force. Fourth, alignment of the implant components and bone models to their segmented points was imperfect. Fifth, bone models and associated muscle and ligament origin and insertion points were taken from a different subject of similar stature. Sixth, EMG measurements were not available to perform a qualitative evaluation of the estimated muscle activation patterns. While these limitations may affect the ultimate goal of estimating *in vivo* muscle and contact forces accurately, they do not prevent investigation of how optimization problem formulation influences calculated muscle and contact forces.

The most significant limitation in the present study is omission of neighboring joints from the model. Seven of the eleven muscles in our model are biarticular, crossing the knee as well as the ankle or hip. However, force-producing constraints imposed on biarticular muscles by neighboring joints were not included in our problem formulations, likely affecting the calculated muscle forces (Fraysse et al., 2009). For example, use of TFL to balance the frontal plane moment at the hip and keep the pelvis level could contribute to increased TFL muscle force and hence increased lateral contact force. Furthermore, some differences in muscle force estimates from the two cost functions can be explained by indeterminacy between uniarticular and biarticular muscles having similar function at the knee (e.g., VAS and RF or BFSH and BFLH). Musculoskeletal modeling software capable of accommodating muscle wrapping surfaces (which Autolev cannot do easily) and user-written contact routines will be needed to extend the current model to include the ankle and hip.

In conclusion, this study presented a novel approach for predicting muscle and contact forces simultaneously in the knee during gait. The approach was made possible by recently developed surrogate contact modeling methods. The "matched" and "predicted" optimization problems demonstrated the abilities and limitations of the current musculoskeletal model based on the magnitudes of the residual loads and the errors in predicted

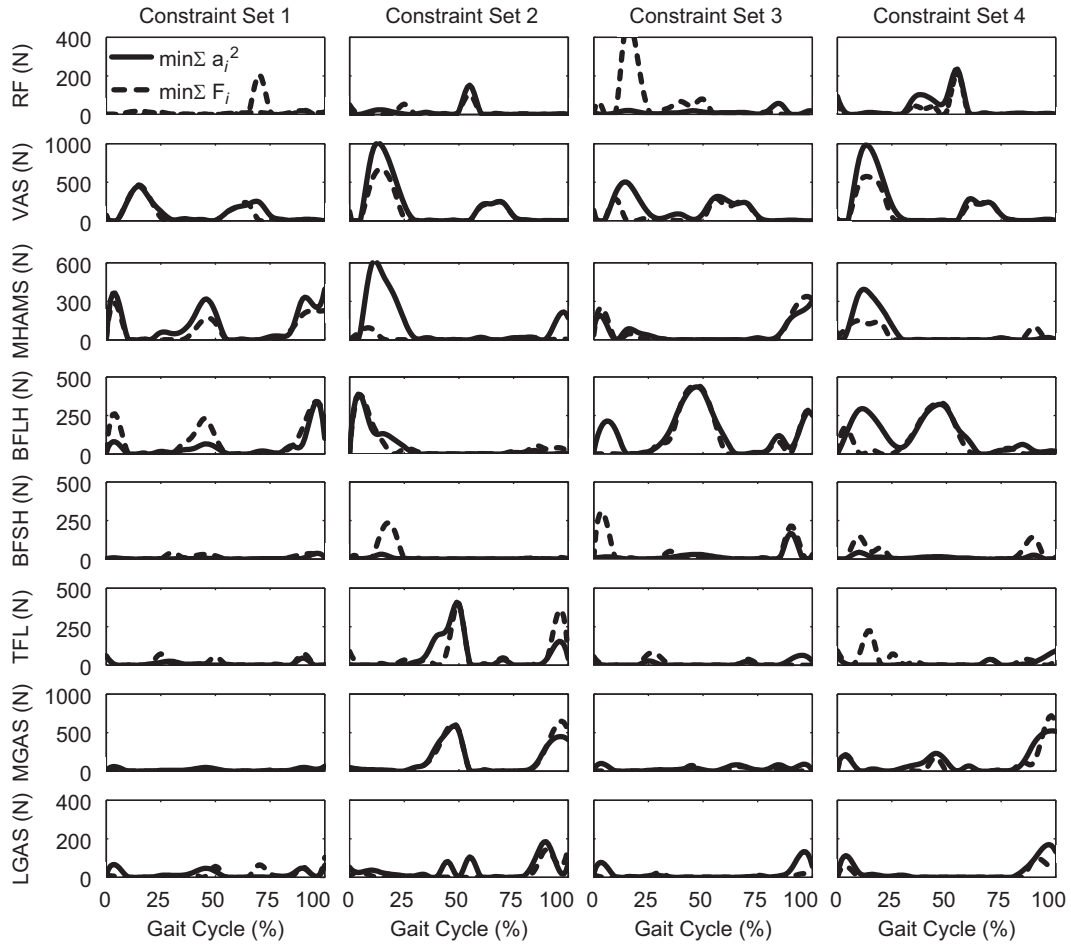

Fig. 7. Estimated muscle forces for the eight "predicted" optimization problems. Each column represents a different constraint set defined in Table 1.

TF contact forces. Demonstrating the feasibility of the simultaneous approach is an important step toward the development of new methods that utilize all available experimental data in the muscle and contact force estimation process for the knee.

Conflict of interest

There are no conflicts of interest.

Acknowledgments

This work was supported by NSF CAREER award CBET0239042 and NSF award CBET0602996 to B.J. Fregly and by Australian Research Council Discovery Project Grant DP0878705 to M.G. Pandy. The authors thank J.W. Fernandez for providing the muscle origin, insertion, and strength data used in this study.

Appendix A. Supporting information

Supplementary data associated with this article can be found in the online version at doi:10.1016/j.jbiomech.2009.10.048.

References

Anderson, F.C., Pandy, M.G., 2001. Static and dynamic optimization solutions for gait are practically equivalent. Journal of Biomechanics 34, 153–161.

Anderson, F.C., Pandy, M.G., 2003. Individual muscle contributions to support in normal walking. Gait and Posture 17, 159–169.

Banks, S.A., Fregly, B.J., Boniforti, F., Reinschmidt, C., Romagnoli, S., 2005. Comparing in vivo kinematics of unicondylar and bi-unicondylar knee replacements. Knee Surgery, Sports Traumatology, Arthroscopy 13, 551–556.

Bei, Y., Fregly, B.J., 2004. Multibody dynamic simulation of knee contact mechanics. Medical Engineering & Physics 26, 777–789.

Besier, T.F., Fredericson, M., Gold, G.E., Beaupre, G.S., Delp, S.L., 2009. Knee muscle forces during walking and running in patellofemoral pain patients and pain-free controls. Journal of Biomechanics 42, 898–905.

Buchanan, T.S., Lloyd, D.G., Manal, K., Besier, T.F., 2005. Estimation of muscle forces and joint moments using a forward–inverse dynamics model. Medicine and Science in Sports Exercise 37, 1911–1916.

Crowninshield, R.D., 1978. Use of optimization techniques to predict muscle forces. Journal of Biomechanical Engineering 100, 88–92.

D'Lima, D.D., Patil, S., Steklov, N., Colwell Jr., C.W., 2007. An ABJS Best Paper: dynamic intraoperative ligament balancing for total knee arthroplasty. Clinical Orthopaedics and Related Research 63, 208–212.

D'Lima, D.D., Patil, S., Steklov, N., Slamin, J.E., Colwell Jr., C.W., 2006. Tibial forces measured in vivo after total knee arthroplasty. Journal of Arthroplasty 21, 255–262.

D'Lima, D.D., Patil, S., Steklov, N., Slamin, J.E., Colwell, C.W.J., 2005a. The Chitranjan Ranawat Award: in vivo knee forces after total knee arthroplasty. Clinical Orthopaedics and Related Research 440, 45–49.

D'Lima, D.D., Townsend, C.P., Arms, S.W., Morris, B.A., Colwell, C.W.J., 2005b. An implantable telemetry device to measure intra-articular tibial forces. Journal of Biomechanics 38, 299–304.

Fraysse, F., Dumas, R., Cheze, L., Wang, X., 2009. Comparison of global and joint-to-joint methods for estimating the hip joint load and the muscle forces during walking. Journal of Biomechanics (in press).

Glitsch, U., Baumann, W., 1997. The three-dimensional determination of internal loads in the lower extremity. Journal of Biomechanics 30, 1123–1131.

Herzog, W., Longino, D., Clark, A., 2003. The role of muscles in joint adaptation and degeneration. Langenbeck's Archives Surgery 388, 305–315.

Jinha, A., Ait-Haddou, R., Herzog, W., 2006. Predictions of co-contraction depend critically on degrees-of-freedom in the musculoskeletal model. Journal of Biomechanics 39, 1145–1152.

Kaufman, K.R., An, K.W., Litchy, W.J., Chao, E.Y., 1991. Physiological prediction of muscle forces – I. Theoretical formulation. Neuroscience Letters 40, 781–792.

Kaufman, K.R., Kovacevic, N., Irby, S.E., Colwell, C.W., 1996. Instrumented implant for measuring tibiofemoral forces. Journal of Biomechanics 29, 667–671.

Kim, H.J., Fernandez, J.W., Akbarshahi, M., Walter, J.P., Fregly, B.J., Pandy, M.G., 2009. Evaluation of predicted knee-joint muscle forces during gait using an instrumented knee implant. Journal of Orthopaedic Research 27, 1326–1331.

Lin, Y.-C., Farr, J., Carter, K., Fregly, B.J., 2006. Response surface optimization for joint contact model evaluation. Journal of Applied Biomechanics 22, 120–130.

Lin, Y.-C., Haftka, R.T., Queipo, N.V., Fregly, B.J., 2008. Dynamic simulation of knee motion using three-dimensional surrogate contact modeling, Proceedings of the 2008 Summer Bioengineering Conference. The American Society of Mechanical Engineers, San Marco Island, Florida SBC2008-190966.

Lin, Y.-C., Haftka, R.T., Queipo, N.V., Fregly, B.J., 2009. Two-dimensional surrogate contact modeling for computationally efficient dynamic simulation of total knee replacements. Journal of Biomechanical Engineering 131, 041010-1–041010-8.

Liu, M.Q., Anderson, F.C., Schwartz, M.H., Delp, S.L., 2008. Muscle contributions to support and progression over a range of walking speeds. Journal of Biomechanics 41, 3243–3252.

Lloyd, D.G., Besier, T.F., 2003. An EMG-driven musculoskeletal model to estimate muscle forces and knee joint moments in vivo. Journal of Biomechanics 36, 765–776.

Neptune, R.R., Zajac, F.E., Kautz, S.A., 2004. Muscle force redistributes segmental power for body progression during walking. Gait and Posture 19, 194–205.

Praemer, A., Furner, S., Rice, D.P., 1999. In: Musculoskeletal Conditions in the United States. American Academy of Orthopaedic Surgeons, Rosemont, IL.

Reeves, N.D., Narici, M.V., Maganaris, C.N., 2003. Strength training alters the viscoelastic properties of tendons in elderly humans. Muscle Nerve 28, 74–81.

Reinbolt, J.A., Haftka, R.T., Chmielewski, T.L., Fregly, B.J., 2008. A computational framework to predict post-treatment outcome for gait-related disorders. Medical Engineering & Physics 30, 434–443.

Reinbolt, J.A., Schutte, J.F., Fregly, B.J., Koh, B.-I., Haftka, R.T., George, A.D., Mitchell, K.H., 2005. Determination of patient-specific multi-joint kinematic models through two-level optimization. Journal of Biomechanics 38, 621–626.

Schultz, A.B., Andersson, G.B.J., 1981. Analysis of loads on the lumbar spine. Spine 6, 76–82.

Sharma, A., Leszko, F., Komistek, R.D., Scuderi, G.R., Cates, H.E.J., Liu, F., 2008. In vivo patellofemoral forces in high flexion total knee arthroplasty. Journal of Biomechanics 41, 642–648.

Shelburne, K.B., Pandy, M.G., Anderson, F.C., Torry, M.R., 2004. Pattern of anterior cruciate ligament force in normal walking. Journal of Biomechanics 37, 797–805.

Shelburne, K.B., Torry, M.R., Pandy, M.G., 2005. Muscle, ligament, and joint-contact forces at the knee during walking. Medicine and Science in Sports and Exercise 37, 1948–1956.

Shelburne, K.B., Torry, M.R., Pandy, M.G., 2006. Contributions of muscles, ligaments, and the ground-reaction force to tibiofemoral joint loading during normal gait. Journal of Orthopaedic Research 24, 1983–1990.

Taylor, W., Heller, M., Bergmann, G., Duda, G., 2004. Tibio-femoral loading during human gait and stair climbing. Journal of Orthopaedic Research 22, 625–632.

Ward, S.R., Powers, C.M., 2004. The influence of patella alta on patellofemoral joint stress during normal and fast walking. Clinical Biomechanics 19, 1040–1047.

Winby, C.R., Lloyd, D.G., Besier, T.F., Kirk, T.B., 2009. Muscle and external load contribution to knee joint contact loads during normal gait. Journal of Biomechanics 42, 2294–2300.

Zhao, D., Banks, S.A., D'Lima, D.D., Colwell Jr., C.W., Fregly, B.J., 2007a. In vivo medial and lateral tibial loads during dynamic and high flexion activities. Journal of Orthopaedic Research 25, 593–602.

Zhao, D., Banks, S.A., Mitchell, K.H., D'Lima, D.D., Colwell, C.W., Fregly, B.J., 2007b. Correlation between the knee adduction torque and medial contact force for a variety of gait patterns. Journal of Orthopaedic Research 25, 789–797.